# Preparation and Enhanced Hydrostability and Hydrogen Storage Capacity of CNT@MOF-5 Hybrid Composite

Seung Jae Yang,[†] Jae Yong Choi,[‡] Hee K. Chae,[‡] Jung Hyun Cho,[†] Kee Suk Nahm,[§] and Chong Rae Park*,[†]

*Carbon Nanomaterials Design Laboratory, Department of Materials Science and Engineering, Seoul National University, Seoul 151-744, Korea, Department of Chemistry Education, Seoul National University, Seoul 151-742, Korea, and Nanomaterial Research Center and School of Chemical Engineering and Technology, Chonbuk National University, Chonju 561-756, Korea*

*Received December 29, 2008. Revised Manuscript Received March 24, 2009*

Metal−organic frameworks (MOFs) are a rapidly growing class of microporous materials. Various MOFs with tailored nanoporosities have recently been developed as potential storage media for natural gases and hydrogen. However, wider applications have been limited because even atmospheric moisture levels cause MOF instability, and unexpectedly low $H_2$ storage capacity, at 298 K. To overcome these problems, we synthesized a hybrid composite of acid-treated multiwalled carbon nanotubes (MWCNTs) and MOF-5 [$Zn_4O(bdc)_3$; bdc = 1,4-benzenedicarbocylate] (denoted MOFMC). In a successful synthesis, well-dispersed MWCNTs in dimethylformamide (DMF) were mixed with a DMF solution of zinc nitrate tetrahydrate and terephthalic acid. The MOFMCs obtained had the same crystal structure and morphology as those of virgin MOF-5, but exhibited a much greater Langmuir specific surface area (increased from 2160 to 3550 $m^2/g$), about a 50% increase in hydrogen storage capacity (from 1.2 to 1.52 wt % at 77 K and 1 bar and from 0.3 to 0.61 wt % at 298 K and 95 bar), and much improved stability in the presence of ambient moisture.

## Introduction

To develop hydrogen-fueled automobiles, a viable $H_2$ storage system is crucial.[1] A variety of materials such as carbon nanotubes (CNTs), zeolites, activated carbons, and complex metal hydrids have been developed as effective $H_2$ storage adsorbents,[2] but none of the materials developed to date are capable of satisfying target criteria set by the United States Department of Energy.[3]

Recently, metal−organic frameworks (MOFs) have been evaluated as promising $H_2$ storage media as MOFs exhibit exceptionally high surface areas and tunable pore size.[4] An additional advantage of MOFs is that preparation is economic as MOFs are synthesized by "one-pot" solvothermal methods under mild conditions. Much effort has been devoted to improving MOF $H_2$ storage capacities[5] and adopting strategies such as high porosity with appropriate pore size, catenation, and inclusion of open metal sites. For example, Rowsell and colleagues attempted to improve $H_2$ storage capacity by tailoring organic ligands.[6a] These authors obtained (at 77 K and 1 bar) $H_2$ storage capacities of 1.62, 1.32, and 1.25 wt % from products with Langmuir specific surface areas (L-SSAs) of 1910, 3360, and 4530 $m^2/g$, respectively. This indicates that high surface area is not the only factor influencing adsorbent $H_2$ storage capacity.[6] Sun and co-workers obtained 1.9 wt % storage at 77 K and 1 bar using interwoven MOFs (of L-SSA 3800 $m^2/g$) in which a single $H_2$ molecule could interact with several ligand aromatic units.[7a] Yaghi and colleagues and Dietzel and co-workers took somewhat different approaches. These authors deliberately introduced open metal sites, or metal centers that were unsaturated in a coordination sense, to increase the affinity of $H_2$ molecules for metal sites.[8] Indeed, MOF-505, which contains such open metal sites, exhibited a much

* Corresponding author. Tel: (+82) 2-880-8030. Fax: (+82) 2-885-1748. E-mail: crpark@snu.ac.kr.
[†] Department of Materials Science and Engineering, Seoul National University.
[‡] Department of Chemistry Education, Seoul National University.
[§] Chonbuk National University.

(1) Schlapbach, L.; Zuttel, A. *Nature (London)* **2001**, *414*, 353.
(2) (a) Hu, J.; Liu, Y.; Wu, G.; Xiong, Z.; Chua, Y. S.; Chen, P. *Chem. Mater.* **2008**, *20*, 4398. (b) Ritschel, M.; Uhlemann, M.; Gutfleisch, O.; Leonhardt, A.; Graff, A.; Taeschner, C. *Appl. Phys. Lett.* **2002**, *80*, 2985. (c) Panella, B.; Hirscher, M.; Roth, S. *Carbon* **2005**, *43*, 2209. (d) Hu, X.; Trudeau, M.; Antonelli, D. M. *Chem. Mater.* **2007**, *19*, 1388. (e) Stphanie-Victoire, F.; Goulay, A. M.; de Lara, E. C. *Langmuir* **1998**, *14*, 7255.
(3) Hydrogen, Fuel Cell & Infrastructure Technologies Program: Multi-year Research, Development, and Demonstration Plan. U.S. Department of Energy, 2005, http://www.eere.energy.gov/hydrogenandfuelcells/mypp/.
(4) (a) Chae, H. K.; Siberio-Perez, D. Y.; Kim, J.; Go, Y. B.; Eddaoudi, M.; Matzger, A. J.; O'Keeffe, M.; Yaghi, O. M. *Nature (London)* **2004**, *427*, 523. (b) Rosi, N. L.; Eckert, J.; Eddaoudi, M.; Vodak, D. T.; Kim, J.; O'Keeffe, M.; Yaghi, O. M. *Science* **2003**, *300*, 1127. (c) Rowsell, J. L. C.; Eckart, J.; Yaghi, O. M. *J. Am. Chem. Soc.* **2005**, *127*, 14904.
(5) Rowsell, J. L. C.; Yaghi, O. M. *Angew. Chem., Int. Ed.* **2005**, *44*, 4670.
(6) (a) Rowsell, J. L. C.; Millward, A. R.; Park, K. S.; Yaghi, O. M. *J. Am. Chem. Soc.* **2004**, *126*, 5666. (b) Pan, L.; Sander, M. B.; Huang, X.; Li, J.; Smith, M.; Bitter, E.; Bockrath, B.; Johnson, J. K. *J. Am. Chem. Soc.* **2004**, *126*, 1308.
(7) (a) Sun, D.; Ma, S.; Ke, Y.; Collins, D. J.; Zhou, H. C. *J. Am. Chem. Soc.* **2006**, *128*, 3896. (b) Chen, B.; Ma, S.; Zapata, F.; Lobkovsky, E. B.; Yang, J. *Inorg. Chem.* **2006**, *45*, 5718.
(8) (a) Chen, B.; Ockwig, N. W.; Millward, A. R.; Contreras, D. S.; Yaghi, O. M. *Angew. Chem., Int. Ed.* **2005**, *44*, 4745. (b) Dinca, M.; Dailly, A.; Liu, Y.; Brown, C. M.; Neumann, D. A.; Long, J. R. *J. Am. Chem. Soc.* **2006**, *128*, 16876. (c) Dietzel, P. D. C.; Panella, B.; Hirscher, M.; Blom, R.; Fjellvag, H. *Chem. Commun.* **2006**, 959.

10.1021/cm803502y CCC: $40.75 
Published on Web 04/17/2009

improved $H_2$ storage capacity of about 2.5 wt % at 77 K and 1 bar.[8a] However, $H_2$ storage by MOFs at room temperature is far below that seen at 77 K and 1 bar. Indeed, interwoven MOFs (with an L-SSA of 303 $m^2/g$) showed 0.3 wt % $H_2$ storage at 298 K and 65 bar,[7b] and Ni-based MOFs containing open metal sites (with an L-SSA of 1083 $m^2/g$) had a $H_2$ storage capacity of 0.3 wt % at 298 K and 90 bar.[8c] Thus, structural modifications such as open metal sites, use of non-zinc metal cores, and higher SSA did indeed contribute to enhanced $H_2$ storage at 77 K, but not necessarily at room temperature.

Among reported MOFs, MOF-5[$Zn_4O(bdc)_3$; bdc = 1,4-benzenedicarboxylate] is the most thermostable, shows the highest porosity, and has a high $H_2$ capacity, suggesting that MOF-5 is a promising gas storage medium, particularly for hydrogen.[9] However, MOF-5 shows relatively low $H_2$ storage capacity at 298 K and is extremely water-sensitive, even under atmospheric conditions, showing a sharp reduction in surface area after prolonged exposure to humid air.[10] If $H_2$ gas adsorption enthalpy and water stability could be improved, MOF-5 would represent a very promising target for commercialization.

Here, we explored a relatively new class of $H_2$ storage media, formed by a combination of acid-treated multiwalled CNTs (MWCNTs; purity > 95% by thermogravimetric analysis; please see Figure S1 in the Supporting Information) and MOF-5. The use of CNTs as composite fillers has been investigated in various applications, and enhanced composite performance has been achieved because of the unusual electroconductive, thermoconductive, mechanical, and hydrophobicity properties of CNTs.[11] In particular, CNTs have been considered as useful composite fillers in $H_2$ storage research. Synergistic effects such as increases in $H_2$ storage capacity, lowered desorption temperature, and reductions in charging and discharging time have been obtained by incorporation of CNTs into $H_2$ storage materials.[12] In this study we incorporated MWCNTs into MOF-5 to prepare a hybrid composite (denoted MOFMC) and found that MOFMC exhibited an enhanced SSA, good $H_2$ storage capacities at both 77 and 298 K over a wide range of pressures, and stability toward ambient moisture.

## Experimental Section

**Reagents and Chemicals.** Zinc nitrate tetrahydrate (Merck), terephthalic acid (Aldrich), *N,N′*-dimethylformamide (Daejung, Korea), and anhydrous chloroform (Aldrich) were used without further purification.

**Preparation of Functionalized MWCNTs and Dispersion in DMF Solution.** MWCNTs (JEIO, Korea) were soaked in mixed acid (a mixture of nitric acid and sulfuric acid) for 24 h at 80 °C with stirring, recovered by filtration, washed with deionized water, and dried at 70 °C (these are denoted a-MWCNTs). Twenty milligrams of a-MWCNTs was dispersed in 20 mL of DMF.

**Preparation of MOF-5.** Zinc nitrate tetrahydrate (0.156 g, 0.6 mmol) and terephthalic acid (0.033 g, 0.2 mmol) were dissolved in 30 mL of DMF in a vial. The reaction mixture was heated in a furnace at 105 °C for 24 h to yield large cubic crystals of MOF-5. The reaction vessel was then removed from the furnace and allowed to cool to room temperature. The cubic crystals were repeatedly washed with DMF and anhydrous chloroform, soaked in anhydrous chloroform for 12 h, filtered, and vacuum-dried under $10^{-3}$ Torr at 150 °C for 24 h.

**Preparation of MOFMC.** a-MWCNTs/DMF (10 mg/10 mL) was mixed with 30 mL of DMF containing predissolved zinc nitrate tetrahydrate (0.156 g) and terephthalic acid (0.033 g), and the resulting mixture was vigorously stirred for 24 h at room temperature. The mixture was heated to 105 °C in a furnace and maintained at that temperature for 24 h without stirring. Cubic crystals, golden in color, were obtained, repeatedly washed with DMF and anhydrous chloroform, and soaked in anhydrous chloroform for 12 h. Further procedures were as described for MOF-5.

**Characterization.** Thermogravimetric analysis (TGA) was carried out under an air/nitrogen flow with a heating rate of 5 °C/min, using an SDT Q 600 instrument (TA Instruments). X-ray photoemission spectroscopy (XPS) (SIGMA PROBE, ThermoVG) was employed to analyze MWCNT surface functional groups. Powder X-ray diffractometry (XRD) was carried out using a D8 Advance (Bruker) diffractometer. Diffractograms were recorded in reflection mode using Ni-filtered Cu Kα radiation ($\lambda = 0.154184$ nm). Light microscopy (Leica) and field-emission scanning electron microscopy (FE-SEM; JSM6330F instrument, JEOL) were used to analyze product morphology. Transmission electron microscopy (TEM; JEM-4010 instrument, JEOL) was employed for microstructure analysis; the accelerating voltage was 400 kV.

**Gas Sorption Measurements.** Gravimetric $H_2$ product adsorption capacities were measured under high-pressure conditions (up to about 95 bar) at 298 K on a magnetic suspension microbalance (Rubotherm), as previously described.[13,14] Volumetric $H_2$ (at 77 and 298 K) and nitrogen adsorption isotherms (at 77 K) up to 1 bar were measured using a Micromeritics ASAP 2020 static volumetric gas adsorption instrument. The nominal error was in the range ±0.00013 wt % for a standard 100 mg sample mass. All sorption isotherms were obtained using gases of ultrahigh purity (99.999%). Before sorption analysis, samples (0.1−0.2 g) in the analysis chamber were subjected to a vacuum of $10^{-5}$ Torr at 150 °C for 12 h. Nonlocal density functional theory (NLDFT) pore size distributions were determined using the cylindrical pore model.

## Results and Discussion

Figure 1 shows FE-SEM and optical micrographs of MOFMC. The MOFMC morphology is characterized by well-defined cubic crystals 50−250 μm in width. The smooth crystal surface (Figure S2) and the black stripes on a transparent golden background (Figure 1b) indicate that CNTs were incorporated inside MOF-5 because virgin

(9) Tsao, C. S.; Yu, M. S.; Chung, T. Y.; Wu, H. C.; Wang, C. Y.; Chang, K. S.; Chen, H. L. *J. Am. Chem. Soc.* **2007**, *129*, 15997.
(10) (a) Kaye, S. S.; Dailly, A.; Yaghi, O. M.; Long, J. R. *J. Am. Chem. Soc.* **2007**, *129*, 14176. (b) Sabo, M.; Henschel, A.; Fröde, H.; Klemm, E.; Kaskel, S. *J. Mater. Chem.* **2007**, *17*, 3827. (c) Greathouse, J. A.; Allendorf, M. D. *J. Am. Chem. Soc.* **2006**, *128*, 10678.
(11) (a) Han, J. T.; Kim, S. Y.; Woo, J. S.; Lee, G.-W. *Adv. Mater.* **2008**, *20*, 3724. (b) Berson, S.; De Bettignies, R.; Bailly, S.; Guillerez, S.; Jousselme, B. *Adv. Funct. Mater.* **2007**, *17*, 3363. (c) Coleman, J. N.; Cadek, M.; Blake, R.; Nicolosi, V.; Ryan, K. P.; Belton, C.; Fonseca, A.; Nagy, J. B.; Gun'ko, Y.; Blau, W. J. *Adv. Funct. Mater.* **2004**, *14*, 791.
(12) (a) Hsieh, C.-T.; Wei, J.-L.; Lin, J.-Y.; Chen, W.-Y. *J. Power Sources* **2008**, *183*, 92. (b) Reddy, A. L. M.; Ramaprabhu, S. *Int. J. Hydrogen Energy* **2007**, *32*, 3998. (c) Wu, C. Z.; Wang, P.; Yao, X.; Liu, C.; Chen, D. M.; Lu, G. Q.; Cheng, H. M. *J. Alloys Compd.* **2006**, *414*, 259.
(13) Lan, A.; Mukasyan, A. *J. Phys. Chem. B* **2005**, *109*, 16011.
(14) Choi, M.; Ryoo, R. *J. Mater. Chem.* **2007**, *17*, 4204.

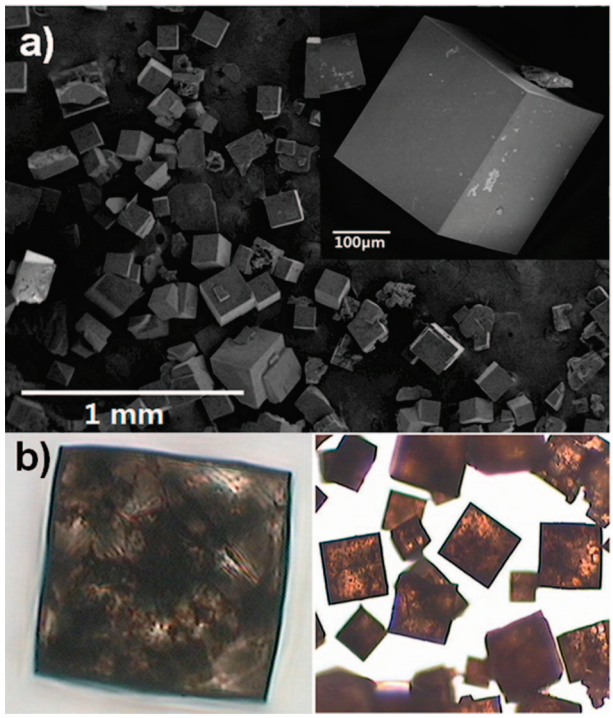


**Figure 1.** (a) FE-SEM micrographs of MOFMC. The inset shows an enlarged view of the crystal. (b) Optical micrographs of MOFMC.

MOF-5 is intrinsically transparent (Figure S3).[15] Powder XRD patterns of virgin MOF-5 and MOFMC (Figure S4) were found to be in perfect agreement with earlier data on MOF-5,[16] confirming that MWCNT incorporation did not disturb or destroy the MOF-5 crystal structure. The characteristic CNT (0 0 2) peak, normally at $2\theta = 26-27°$, was swamped by high-intensity MOF-5 peaks. However, TEM (Figure 2) revealed that MWCNTs were indeed well admixed with MOF-5 crystallites and the hybrid composite thus showed an electron diffraction pattern consisting of the (0 0 2) reflection of MWCNTs and the (12 2 0) reflection of MOF-5 (Figure 2c). High-resolution hybrid composite lattice images (Figure 2a,b) also showed two distinctive lattice spacings of 0.33 and 0.21 nm, corresponding to interlayer spacing values for the (0 0 2) plane of MWCNTs and the (12 2 0) plane of MOF-5, respectively. It is generally accepted that MOF-5 crystals are very susceptible to electron beams, making it near impossible to view a lattice image, or even to measure the MOF-5 electron diffraction pattern in a selected area, using TEM.[17] However, we successfully obtained from MOFMC, for the first time, a high-resolution lattice image of MOF-5 crystals. This is presumably because the incorporated MWCNTs sustain the MOFMC crystal structure by dissipating electrostatic charges accumulating under electron beam dosage.

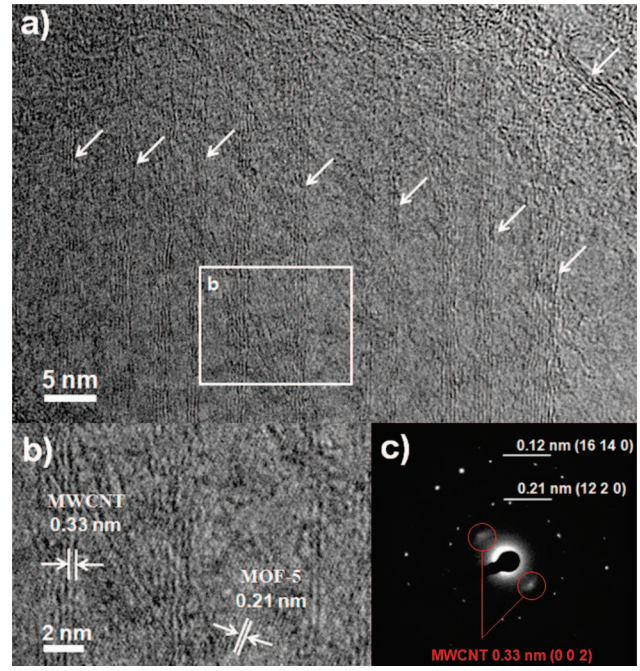


**Figure 2.** (a) HRTEM micrograph of an MOFMC crystal (white arrows indicate MWCNT lattices). (b) Enlarged view of the boxed area in (a), and (c) typical selected area electron diffraction patterns of (a).

**Table 1. Nitrogen Adsorption Properties of MWCNTs, MOF-5, and MOFMC**

| material | nitrogen uptake[a] [mmol/g] | BET SSA[b] [$m^2$/g] | Langmuir SSA[b] [$m^2$/g] | pore vol (<1 nm)[c] [$cm^3$/g] | pore vol (>1 nm)[c] [$cm^3$/g] |
|---|---|---|---|---|---|
| MWCNT | 17.8 | 147 | 202 | | |
| MOF-5 | 23.3 | 1810 | 2160 | 0.271 | 0.552 |
| MOFMC | 37.3 | 2900 | 3550 | 0.672 | 0.765 |

[a] Maximum uptake observed at 77 K. [b] SSA = specific surface area, determined using the BET and Langmuir equations. [c] Determined by NLDFT pore size distribution.

Table 1 lists the L-SSAs of MWCNTs, MOF-5, and MOFMC, as determined from $N_2$ adsorption isotherms at 77 K (Figure S5). It is noteworthy that MWCNT incorporation increased L-SSA from 2160 (MOF-5) to 3550 (MOFMC) $m^2$/g. It has been reported that MOF-5 samples prepared from DMF solution generally show L-SSAs in the range 1000−2500 $m^2$/g whereas materials prepared from diethylformamide (DEF) solutions have L-SSAs of 3100−4000 $m^2$/g.[9,15a] Thus, it appears that the MOFMC L-SSA obtained is the highest reported for DMF solvent-based MOF-5s. Figure 3 shows the pore size distributions (PSDs) of MOF-5 and MOFMC calculated using NLDFT. The two materials showed typical type I isotherm nitrogen adsorption and may be regarded as having only micropores (pore width < 2 nm); the PSD data can be divided into two regimes with pore sizes of 0.5−0.9 nm (I) and 1.3−1.5 nm (II). These two classes reflect the role of incorporated MWCNTs in pore activation. According to Tsao and colleagues,[9] a stable pore network structure is critical for solvent (DMF, DEF, and chloroform) removal during pore activation to produce MOF-5s of high SSAs, and collapse of the pore network structure during pore activation results in a relatively low SSA. The similarity of the two PSDs (Figure 3a) in regime II indicates that enhancement in the surface area of the hybrid

(15) (a) Hafizovic, J.; Bjørgen, M.; Olsbye, U.; Dietzel, P. D. C.; Bordiga, S.; Prestipino, C.; Lamberti, C.; Lillerud, K. P. *J. Am. Chem. Soc.* **2007**, *129*, 3612. (b) Grzesiak, A. L.; Uribe, F. J.; Ockwig, N. W.; Yaghi, O. M.; Matzger, A. J. *Angew. Chem., Int. Ed.* **2006**, *45*, 2553.
(16) Panella, B.; Hirscher, M.; Pütter, H.; Müller, U. *Adv. Funct. Mater.* **2006**, *16*, 520.
(17) (a) Lebedev, O. I.; Millange, F.; Serre, C.; Van Tendeloo, G.; Ferey, G. *Chem. Mater.* **2005**, *17*, 6525. (b) Schröder, F.; Esken, D.; Cokoja, M.; van den Berg, M. W. E.; Lebedev, O. I.; Van Tendeloo, G.; Walaszek, B.; Buntkowsky, G.; Limbach, H.-H.; Chaudret, B.; Fischer, R. A. *J. Am. Chem. Soc.* **2008**, *130*, 6119. (c) Hermes, S.; Marie-Katrin Schröter, M.; Schmid, R.; Khodeir, L.; Muhler, M.; Tissler, A.; Fischer, R. W.; Fischer, R. A. *Angew. Chem., Int. Ed.* **2005**, *44*, 623.

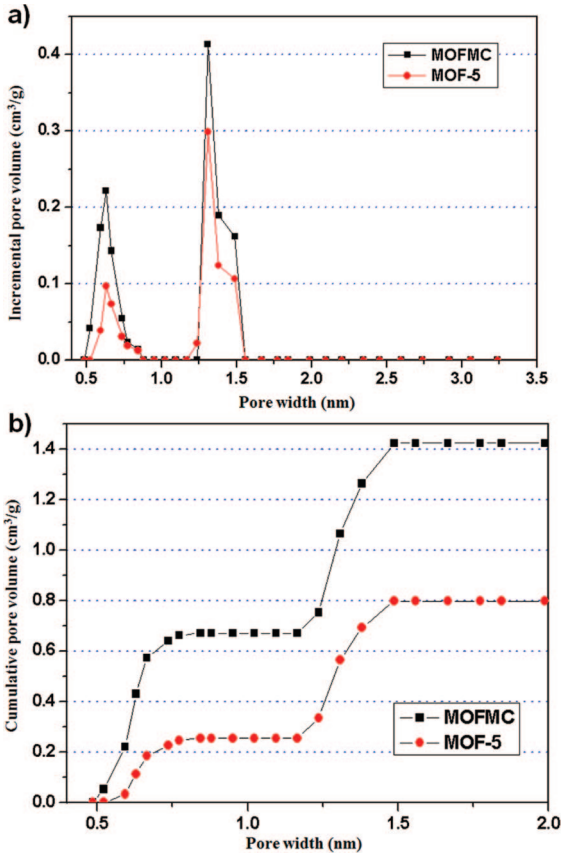


**Figure 3.** Nonlocal density functional theory (NLDFT) pore size distributions of products by (a) incremental pore volume and (b) cumulative pore volume.

composites (MOFMC) is possibly due to the incorporated MWCNTs, which help to secure effective solvent diffusion paths or assist in removal of impurities (such as unreacted zinc species) during pore activation. The TGA data (Figure S6) confirm that incorporated MWCNTs facilitate pore activation. Solvent is removed from MOFMC at a much lower temperature (132 °C) than is required during MOF-5 preparation (248 °C), and more solvent was removed from MOFMC over any given time or at any tested temperature, because of larger pore volume. Furthermore, MWCNTs in MOFMC enhanced thermal stability, as confirmed by a rise in decomposition temperature from 452 to 492 °C. The additional ultramicropores (mainly 0.7 nm in diameter) may be the result of MWCNT incorporation. This is supported by the observation that the increase in regime I pores (from 0.271 to 0.672 $cm^3/g$; 2.48-fold) was much higher than that of regime II pores (from 0.552 to 0.765 $cm^3/g$; about 1.386-fold). When the regime II proportions were considered, it was found that MOFMC regime I ultramicropores had an additional volume of about 0.3 $cm^3/g$, arising from incorporated MWCNTs. Some recent studies have disclosed that MOF substrates with surface carboxylate functional groups form MOFs by heterogeneous nucleation and crystal growth because carboxylate groups act as nucleation sites.[18] Thus, we treated MWCNTs with a mixture of nitric acid and sulfuric acid (1:3, v/v) to introduce a maximal level of surface MWCNT carboxylic

(18) (a) Shoaee, M.; Anderson, M. W.; Attfield, M. P. *Angew. Chem., Int. Ed.* **2008**, *47*, 8525. (b) Scherb, C.; Schödel, A.; Bein, T. *Angew. Chem., Int. Ed.* **2008**, *47*, 5777. (c) Hermes, S.; Schröder, F.; Chelmowski, R.; Wöll, C.; Fischer, R. A. *J. Am. Chem. Soc.* **2005**, *127*, 13744.

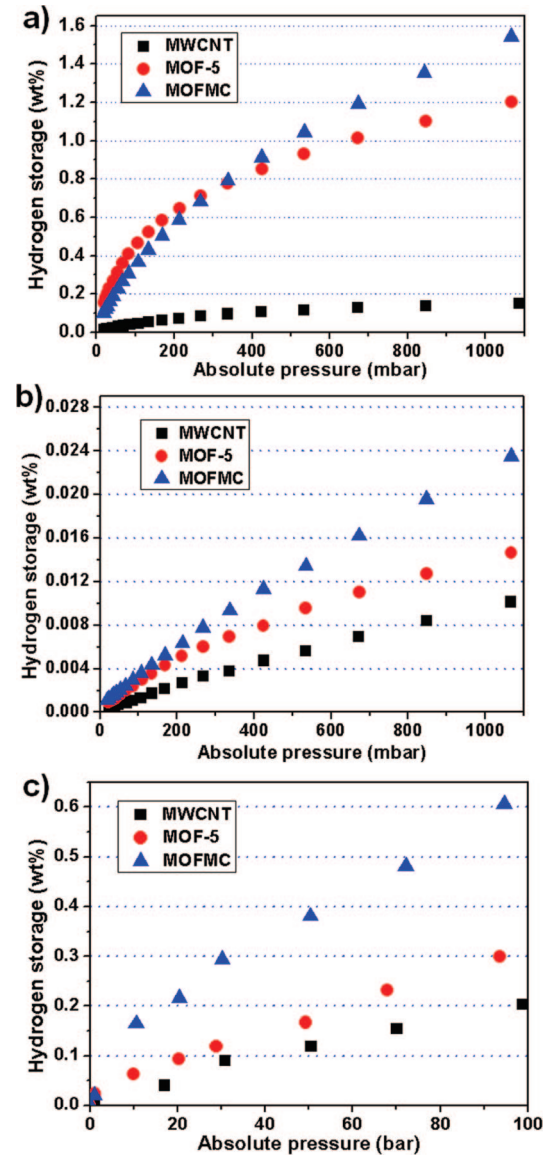


**Figure 4.** Low-pressure $H_2$ adsorption capacity measured volumetrically at (a) 77 K and (b) 298 K and (c) high-pressure $H_2$ adsorption capacity measured gravimetrically at 298 K, of MWCNTs, MOF-5, and MOFMC.

groups, as confirmed by XPS (Figure S7). We therefore believe that our MOF crystals were formed by heteronucleation and crystal growth on MWCNT carboxylic groups, and interface ultramicropores might thus exist. However, it is very difficult to characterize the interface region separately using presently available tools, and interface formation is difficult to define with precision. This is why earlier work showed only a schematic of the proposed mechanism.[18] It may be reasonable to suggest that regimes I and II are related to inducing additional ultramicropore development in the interface between the two materials and offering a conduit for removal of solvent or impurities during pore activation.

The $H_2$ adsorption behaviors of samples at 77 and 298 K are shown in Figure 4. MWCNTs and MOF-5 exhibited $H_2$ uptakes of 0.15 and 1.2 wt %, respectively, in good agreement with previous studies,[6a] but MOFMC showed a somewhat increased capacity of 1.52 wt % at 77 K and 1 bar (Figure 4a). Generally, it is recognized that ultramicropores 0.6−0.7 nm in diameter are more effective in high-

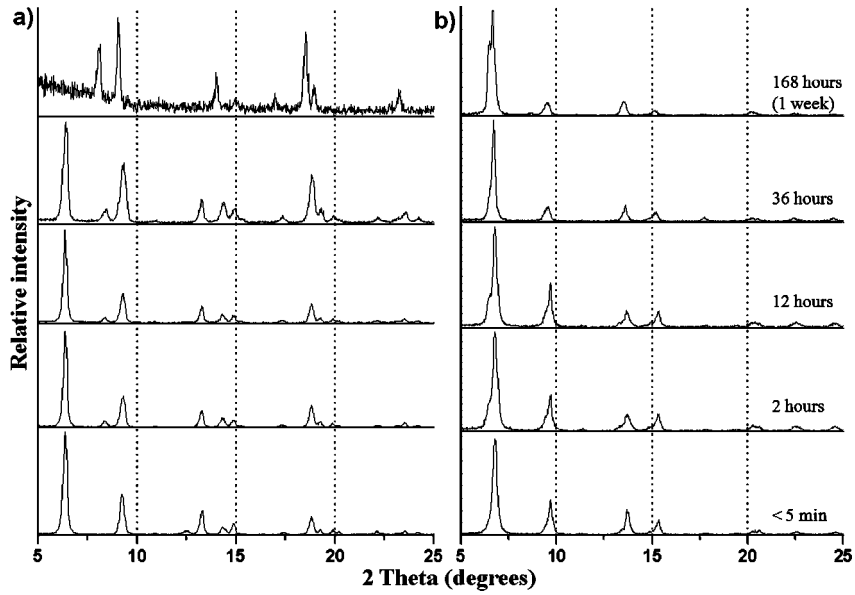


**Figure 5.** Powder X-ray diffraction patterns for (a) MOF-5 and (b) MOFMC exposed to static air conditions (23 °C and 33% relative humidity) for <5 min, 2 h, 12 h, 36 h, and 168 h.

level hydrogen uptake than are pores of other diameters.[19] In MOF-5s, extremely high SSAs (over 3000 $m^2/g$ from DEF-based syntheses) are obtained, but pore diameter is usually 1.2−1.3 nm.[20] This is why relatively low hydrogen uptakes of 1.2−1.3 wt % at 77 K (1 bar) and 0.3−0.4 wt % at 298 K (100 bar) are seen, despite high SSAs.[6a,16,21] With MOFMCs, the ultramicropore volume was significantly increased compared with that of MOF-5s, although MOFMCs' crystal structure was the same as that of MOF-5. Thus, the 1.52 wt % $H_2$ storage capacity of MOFMC contains a contribution from ultramicropores arising because of MWCNT incorporation. It is particularly noteworthy that, at 298 K and high pressure, the hybrid composite $H_2$ storage capacity became much more apparent. At low pressure and 298 K (Figure 4b), $H_2$ storage capacity of MOFMC was only slightly higher than those of other materials examined (MOFMC, 0.024 wt %; MOF-5, 0.015 wt %; MWCNT, 0.010 wt %), and the MOFMC isotherm slope indeed suggested enhanced $H_2$ storage capacity at high pressure. Under higher pressure, up to about 95 bar at 298 K (Figure 4c), MWCNTs and MOF-5 had $H_2$ storage capacities of 0.2 and 0.3 wt %, almost the same as in previous reports.[9,13,16] However, the hybrid composite had a twofold greater $H_2$ storage capacity (0.61 wt %) than did MOF-5. Furthermore, adsorption at each tested pressure was reversible, and equilibrium was obtained within 10 min (data not shown). These observations imply that additional micropore development within MOFMC enhanced $H_2$ storage capacity at 77 K, but particularly at 298 K, over a wide pressure range.

An interesting feature of the MOF-5/MWCNT hybrid composite is enhanced moisture stability under ambient conditions. Moisture stability tests on MOF-5 and MOFMC were carried out at 33% relative humidity and 23 °C (Figure 5). Exposure of desolvated MOF-5 to air for 2 h resulted in the appearance of a new XRD peak at around 8.4°, indicating commencement of decomposition.[10] On subsequent exposure to air, peak relative intensity increased, indicating acceleration of decomposition.[10] After 1 week of air exposure, decomposition was almost complete, as no MOF-5 crystal reflections were seen. However, even after 1 week in air, the reflections of MOFMC did not change. Thus, we believe that incorporation of MWCNTs into MOF-5 crystals protects the moisture-sensitive MOF-5 surface, now covered (at least partially) with rigid MWCNTs.

## Conclusion

In conclusion, we successfully synthesized a novel hybrid composite designated CNT@MOF-5 (MOFMC) and found significant SSA enhancement, improvement in $H_2$ storage capacity at room temperature, and increased moisture stability, compared with those of MOF-5. These very useful results suggest a new approach to increasing MOF hydrogen adsorption enthalpy, utilizing zinc-based MOFs in humid air without loss of surface area. This approach also presents a new direction for achieving novel hybrid materials between the two spotlighting materials, viz. CNTs and MOF-5.

**Acknowledgment.** This work was supported by the "National RD&D Organization for Hydrogen & Fuel Cell" and the "Ministry of Knowledge and Economy" of Korea.

**Supporting Information Available:** TGA thermograms of MWCNTs, MOF-5, and MOFMC; FE-SEM micrographs of MOFMC; light micrographs of MOF-5 and MOFMC; X-ray diffractograms of MOF-5 and MOFMC; nitrogen adsorption isotherms at 77 K of MWCNTs, MOF-5, and MOFMC; XPS spectra of acid-treated and untreated MWCNTs. This material is available free of charge via the Internet at http://pubs.acs.org.

CM803502Y

(19) (a) Yushin, G.; Dash, R.; Jagiello, J.; Fischer, J. E.; Gogotsi, Y. *Adv. Funct. Mater.* **2006**, *16*, 2288. (b) Cabria, I.; Lúpez, M. J.; Alonso, J. A. *Carbon* **2007**, *45*, 2649.
(20) Yaghi, O. M.; O'Keeffe, M.; Ockwig, N. W.; Chae, H. K.; Eddaoudi, M.; Kim, J. *Nature (London)* **2003**, *423*, 705.
(21) Panella, B.; Hirscher, M. *Adv. Mater.* **2005**, *17*, 538.